

# An Ionizable Active-Site Tryptophan Imparts Catalase Activity to a Peroxidase Core

Peter C. Loewen,<sup>†,⊗</sup> Xavi Carpena,<sup>‡,⊗</sup> Pietro Vidossich,<sup>§,⊗</sup> Ignacio Fita,<sup>\*,†,⊗</sup> and Carme Rovira<sup>\*,||,⊗</sup>

<sup>†</sup>Department of Microbiology, University of Manitoba, Winnipeg MB R3T 2N2, Canada

<sup>‡</sup>IRB Barcelona, <sup>†</sup>Institut de Biologia Molecular de Barcelona (IBMB-CSIC), Parc Científic de Barcelona, Baldori Reixac 10-12, 08028 Barcelona, Spain

<sup>§</sup>Departament de Química, Edifici Cn., Universitat Autònoma de Barcelona, 08193 Cerdanyola del Vallès, Spain

<sup>||</sup>Departament de Química Orgànica and Institut de Química Teòrica i Computacional (IQTUCUB), Universitat de Barcelona, Martí i Franquès 1, 08028 Barcelona, Spain

<sup>#</sup>Institució Catalana de Recerca i Estudis Avançats (ICREA), Passeig Lluís Companys, 23, 08020 Barcelona, Spain

## Supporting Information

**ABSTRACT:** Catalase peroxidases (KatG's) are bifunctional heme proteins that can disproportionate hydrogen peroxide (catalatic reaction) despite their structural dissimilarity with monofunctional catalases. Using X-ray crystallography and QM/MM calculations, we demonstrate that the catalatic reaction of KatG's involves deprotonation of the active-site Trp, which plays a role similar to that of the distal His in monofunctional catalases. The interaction of a nearby mobile arginine with the distal Met-Tyr-Trp essential adduct (in/out) acts as an electronic switch, triggering deprotonation of the adduct Trp.

Catalase peroxidases (KatG's) are heme proteins capable of a fascinating diversity of reactions, most notably the conversion of the widely used anti-tubercular pro-drug isonicotinic acid hydrazide (isoniazid or INH) to its active form, isonicotinyl-NAD.<sup>1</sup> KatG's are characterized as broad substrate range peroxidases with also a high catalase (catalatic) activity ( $2\text{H}_2\text{O}_2 \rightarrow 2\text{H}_2\text{O} + \text{O}_2$ ).<sup>2</sup> The heme-containing reaction center of KatG<sup>3</sup> closely resembles that of peroxidases such as cytochrome *c* peroxidase (CCP) and ascorbate peroxidase (APX).<sup>4</sup> However, while the catalatic activity of peroxidases is very low (or totally absent),<sup>5</sup> the catalatic activity in KatG's is  $\sim 2\text{--}3$  orders of magnitude higher than its peroxidatic activity.<sup>5a,6</sup> Rationalizing this unusual behavior remains a most intriguing question in peroxidase chemistry.<sup>5a,7</sup>

Despite the active center similarities between KatG and peroxidases, there are a few features that are specific to KatG. The most conspicuous is a covalent adduct (M-W-Y) between a methionine, a tyrosine and a tryptophan stacked 3.4 Å above the heme (Figure 1). This tryptophan often displays a perhydroxy modification on the indole (W-OOH, Figure 1),<sup>8</sup> attributed to reaction of KatG with oxygen.<sup>9</sup> The importance of the M-Y-W adduct is evident in mutations, causing a complete loss of catalase activity.<sup>10</sup> Near this unique adduct, a mobile arginine alternates *in* and *out* of an interaction with the adduct Tyr (Figure 1).<sup>8a,11</sup> The role of this arginine is particularly enigmatic because it is not in direct contact with the heme (the  $\text{C}_\alpha$  is about 20 Å away from the

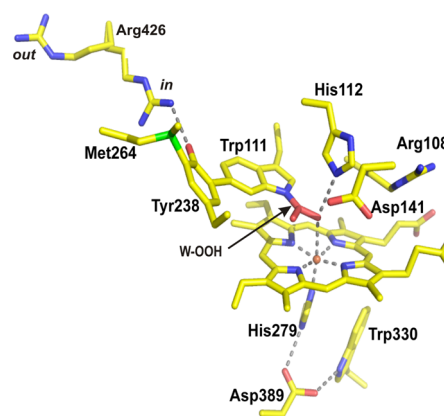


**Figure 1.** Heme cavity of KatG (1MWV). The two conformations of the mobile arginine (Arg426, BpKatG numbering is used) are highlighted.

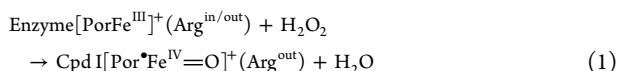
heme iron), but its mutation reduces catalase activity by >95%.<sup>8a</sup> Due to the mobility of the arginine, the adduct Tyr exhibits a  $\text{pK}_a$  significantly lower ( $\sim 6.5$ )<sup>8a,12</sup> than that of a normal tyrosine, being found as either protonated (Y-OH) or unprotonated (Y-O<sup>-</sup>) at neutral pH. In the Y-OH state, the mobile Arg exhibits the *out* conformation, while in the unprotonated Y-O<sup>-</sup> state, the Arg adopts the *in* conformation, forming an ionic Y-O<sup>-</sup>...Arg interaction (Figure 1).<sup>8a,11b,12</sup> Obviously, a molecular model of the reaction mechanism of KatG must explain the roles of all these actors.

Figure S1 (Supporting Information) summarizes the overall reaction cycle of KatG, with special emphasis on the protonation state of the adduct Tyr and Arg conformation. The first stage in both the catalase and peroxidase reactions involves heme oxidation by one molecule of  $\text{H}_2\text{O}_2$  to form Compound I (Cpd I), with the heme iron oxidized to the  $\text{Fe}^{\text{IV}}$  state and a second oxidizing equivalent stored as a porphyrin radical (reaction 1). The mobile arginine is known to fully adopt the *out* conformation in Cpd I.<sup>11b</sup> Thus, formation of Cpd I is

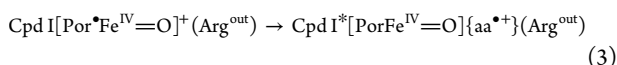
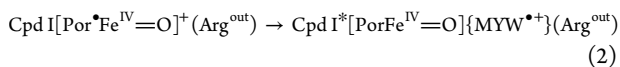
Received: March 25, 2014

Published: May 2, 2014

concomitant with swinging of the arginine from the *in* to the *out* conformation for the  $Y-O^-$  state (Figure S1, top).

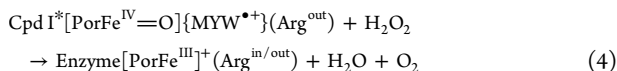


It has been shown that the porphyrin radical of KatG Cpd I is rather unstable<sup>12</sup> and rapidly migrates either to the MYW adduct, forming MYW $\cdot^+$  (reaction 2), or to a distant protein residue<sup>14</sup> (reaction 3). (We use the standard notation Cpd I/Cpd I $\cdot^*$  to indicate whether the radical is on the porphyrin or on a protein amino acid, respectively.)



In the first case (reaction 2), the adduct Tyr must be unprotonated, as this is the only KatG state in which the adduct radical is stable.<sup>12</sup> As previously demonstrated, the ionization potential of the adduct tyrosine decreases considerably when Tyr is unprotonated and Arg does not interact with it (Arg $^{\text{out}}$ ). This triggers fast electron transfer to the porphyrin, stabilizing the radical adduct.<sup>12</sup> This type of Cpd I $\cdot^*$  (reaction 2 and Figure S1, c), predicted on the basis of QM/MM calculations,<sup>12</sup> was recently characterized experimentally.<sup>15</sup> Notably, closely related monofunctional peroxidases, such as CCP, with a structurally equivalent distal tryptophan but lacking both the covalent adduct and the mobile arginine, do not form a radical on any distal residue.<sup>16</sup> Thus, it is reasonable to assume that *the formation of this unique form of Cpd I $\cdot^*$ {PorFe $^{\text{IV}}$ =O}{MYW $\cdot^+$ }(Arg $^{\text{out}}$ ) is what imparts catalase activity to KatG's; thus, it can be termed "catalatic Cpd I $\cdot^*$ ".*

To complete the catalase reaction, Cpd I $\cdot^*$  must be reduced by a second molecule of H $_2$ O $_2$  (Figure S1, catalase pathway):



It is in this second stage where the major difference between KatG and peroxidases emerges, as only KatG is able to reduce Cpd I efficiently. In this regard, it is useful to recall the recently elucidated mechanism of monofunctional catalases.<sup>13</sup> Here, Cpd I reduction by H $_2$ O $_2$  starts by the abstraction of a peroxide hydrogen atom (Figure 2), followed by proton transfer mediated

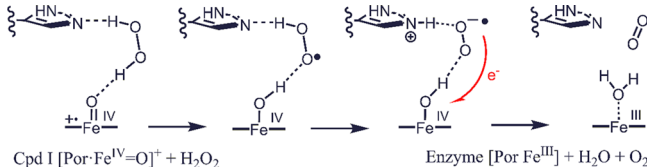


**Figure 2.** Reduction of Cpd I in monofunctional catalases.<sup>13</sup>

by the distal histidine. How can KatG, with its peroxidase-like active site, undergo a mechanism that emulates the efficiency of monofunctional catalases?

In KatG, the distal His (His112 in Figure 1) lies perpendicular to the heme (Figure 1); thus, it is not well oriented to act as an acid/base residue in this step of the reaction. In contrast, the adduct Trp (Trp111 in Figure 1), with its indole N-H group pointing in toward the upper face of the heme, is in a good position to play this role (Figures 1 and 3a). This naturally leads

to the question, can the adduct Trp play an active role in the catalytic reaction in KatG similar to the role played by the distal histidine in catalases? The high  $pK_a$  of its indole proton ( $\sim 16$ ) makes it very unlikely. However, the adduct Trp exhibits radical character in catalytic Cpd I $\cdot^*$ {PorFe $^{\text{IV}}$ =O}{MYW $\cdot^+$ }(Arg $^{\text{out}}$ ), which is expected to lower its  $pK_a$  considerably.<sup>17</sup> In fact, an extreme drop in  $pK_a$ , up to  $\sim 4$ , has been observed for radical tryptophans.<sup>18</sup> Moreover, a high reactivity of the adduct Trp can be inferred from KatG X-ray structures, often displaying a W-OOH modification (Figure 1).<sup>11</sup> Thus, a mechanism with the adduct Trp playing a role similar to that of the distal histidine in catalases becomes plausible.

The possible participation of the adduct Trp in Cpd I reduction was tested by Car-Parrinello QM/MM calculations,<sup>19</sup> based on Density Functional Theory (DFT), plus structure optimizations to scan the proton-transfer coordinate (Figure 3 and S1). First, a molecule of H $_2$ O $_2$  was placed in the active site of KatG Cpd I, and its orientation was explored by QM/MM molecular dynamics (MD). The most favored structure of the Cpd I $\cdot^*$ ...H $_2$ O $_2$  complex (Figure 3a) is one in which the peroxide forms hydrogen bonds with both the distal His and the oxoferryl oxygen of Cpd I. In this orientation, there is a very short O...O distance (2.65 Å) between the oxoferryl oxygen and one peroxide oxygen atom. This is indicative of a facile hydrogen atom transfer,<sup>13,20</sup> involving an energy barrier  $\leq 5$  kcal/mol. The optimized structure and spin distribution after hydrogen atom transfer (Figure 3b and Table S2) confirm the presence of a peroxy radical (HO $_2\cdot$ ) and an Fe $^{\text{III}}$ -OH species, together with an adduct radical. The increase of the Fe-O distance on going from an Fe=O to an Fe-OH bond (A $\rightarrow$ B) brings the hydroxoferryl oxygen closer to the Trp indole hydrogen (the N $_{\text{Trp}}$ -H...O distance decreases from 2.33 to 2.01 Å). This facilitates the subsequent transfer of the Trp indole proton, a process that generates one water molecule (Figure 3c). The low energy barrier observed (12.5 kcal/mol), similar to that obtained for monofunctional catalases,<sup>13</sup> indicates that proton transfer via Trp in KatG is feasible.

The two radicals (HO $_2\cdot$  and the adduct {MYW $\cdot^+$ }, Figure 3c) in close proximity ( $\sim 3$  Å) in the active site of KatG can readily couple, forming the perhydroxy modification of the MYW adduct (W-OOH). To prove that the W-OOH modification is indeed part of the catalytic cycle of KatG's, a 1.8 Å data set was collected from a crystal of BpKatG soaked in a 25 mM H $_2$ O $_2$  solution until oxygen evolution from the crystal was evident. Significantly, the heme cavity is dominated by the MYW adduct modification W-OOH (Figure 4a, Table S1), whereas a control crystal soaked with peracetic acid lacks the modification. Thus, we conclude that the Trp perhydroxy modification is present as a discrete species in catalytically active crystals.

Intriguingly, W-OOH is observed in two conformations (Figure 1), depending on whether the perhydroxy group interacts with the distal His imidazole and the heme iron. The first conformation is the dominant one in active crystals soaked with H $_2$ O $_2$  (Figure 4a, Table S1). Instead, the second conformation is the only one found in the inactive variant D141A (Figures 4b and S1), suggesting that the conformation of the Trp perhydroxy modification is important for the reaction to proceed.

The structural and QM/MM results presented here, together with the available experimental and theoretical information, allow us to formulate a novel molecular mechanism for the catalytic reaction in KatG that explains for the first time the roles of the mobile Arg and the MYW adduct. Specifically, the *catalase*

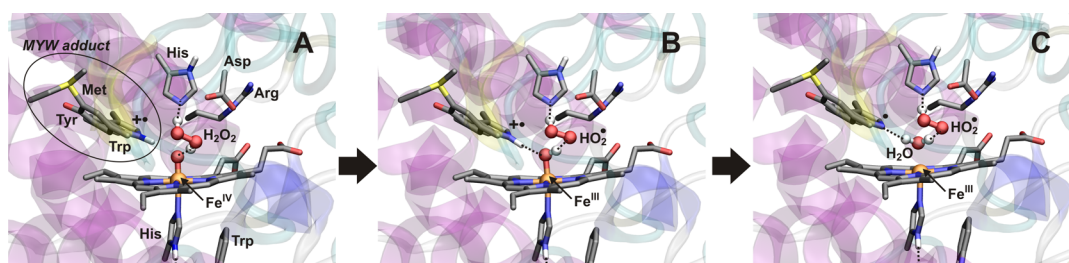


**Figure 3.** Formation of a water molecule during the catalytic reduction of Cpd I in KatG. Calculations were performed at the QM(B3LYP)/MM level of theory (see SI for details). The QM subsystem is shown in licorice and ball-and-stick representation. Water molecules and H atoms are omitted for clarity, except those of H<sub>2</sub>O<sub>2</sub>, H<sub>2</sub>O, and the N–H bonds of Trp and His.

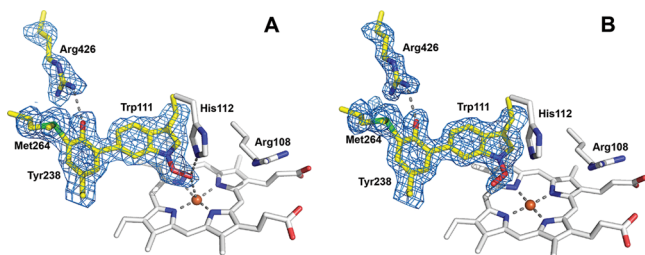


**Figure 4.** Electron density maps of (A) a catalytically active crystal, soaked for 30 s in 25 mM H<sub>2</sub>O<sub>2</sub>, at pH ~6.0 and (B) a crystal of D141A at pH 6.2 (Table S1). The F<sub>o</sub> – F<sub>c</sub> omit electron density maps drawn at  $\sigma = 5.0$  in blue were calculated without the side chains of Trp111, Tyr238, Met264, Arg426, or the W–OOH modification.

branch of the KatG catalytic cycle (Figure S1) involves the following steps (see Figure 5):

(1) *Formation of Cpd I* [Por<sup>•</sup>Fe<sup>IV</sup>=O]<sup>+</sup> (species **b**) by reaction of the Fe<sup>III</sup>-heme with one molecule of H<sub>2</sub>O<sub>2</sub>.

(2) *Formation of Cpd I\** [PorFe<sup>IV</sup>=O]{MYW<sup>•+</sup>} by one-electron transfer from the MYW adduct to the heme. The interaction between Tyr–O<sup>–</sup> and the mobile Arg is repulsive when the MYW adduct holds a radical;<sup>12</sup> thus, formation of {MYW<sup>•+</sup>} is concomitant with switching of the Arg from *in* to *out* (a→c in Figure 5). In other words, conformation *out* stabilizes the radical adduct, whereas conformation *in* precludes formation of the adduct radical.

(3) *Binding of a second molecule of H<sub>2</sub>O<sub>2</sub>* (d in Figure 5). As observed in the QM/MM calculations, the MYW adduct remains in its radical state upon H<sub>2</sub>O<sub>2</sub> binding.

(4) *Hydrogen atom transfer from H<sub>2</sub>O<sub>2</sub> to Cpd I\**. Similarly to monofunctional catalases,<sup>13</sup> a hydrogen atom is transferred from H<sub>2</sub>O<sub>2</sub> to the oxoferryl oxygen, forming a peroxy radical (HO<sub>2</sub><sup>•</sup>). In monofunctional catalases, because of the presence of a porphyrin radical, this leads to the formation of a Por Fe<sup>IV</sup>-OH species. In KatG, since the electron equivalent is stored in the

MYW adduct, such a H-transfer process leads to the formation of a ferric species, [Por Fe<sup>III</sup>-OH]{MYW<sup>•+</sup>} (e in Figure 5).

(5) *Proton transfer* from the adduct Trp to the hydroxoferryl oxygen (e→f), resulting in the formation of one water molecule (Figure 3c).

(6) *Radical coupling*. The two radicals, MYW<sup>•+</sup> and HO<sub>2</sub><sup>•</sup>, readily couple, forming the W-OOH modification. At this stage (g in Figure 5), one of the oxygen atoms of the –OOH group interacts with the heme iron while maintaining its interaction with the distal His (Figure 4a). This is consistent with such a conformation being observed in catalytically active crystals, whereas the reaction cannot proceed in mutants exhibiting the alternative conformation (Figure 4b). After formation of the W-OOH modification, the MYW adduct no longer holds a radical. Thus, the mobile Arg swings to the *in* conformation (g).

(7) *Formation of an Fe<sup>III</sup>-O<sub>2</sub><sup>•–</sup> species*. Breaking of the N(Trp)–OOH bond leads to the formation of a ferric superoxo species (Fe<sup>III</sup>-O<sub>2</sub><sup>•–</sup>) and an adduct radical (h in Figure 5). This is the reverse of the previously investigated oxygen activation process of KatG.<sup>9</sup> Interestingly, oxygen binding was found to be an endothermic process; thus, it is favored in the h→a direction. This is also consistent with the recent spectroscopic detection of a species described as compound III (Cpd III, with formula Fe<sup>III</sup>-O<sub>2</sub><sup>•–</sup>, or its isoelectronic Fe<sup>II</sup>-O<sub>2</sub> form) in active KatG's.<sup>5b,7a,b,15b</sup> The fact that a high H<sub>2</sub>O<sub>2</sub> concentration had to be used<sup>21</sup> suggests that h is a transient species.

(8) *Oxygen generation*. Previous work<sup>9</sup> showed that molecular oxygen may coordinate to Fe upon electron transfer from the MYW adduct. Invoking microreversibility, electron transfer from Fe<sup>III</sup>-O<sub>2</sub><sup>•–</sup> to the MYW adduct radical leads to the resting state of the enzyme. It is evident from Figure 5 that the two oxygen atoms of the released oxygen molecule originate from the second H<sub>2</sub>O<sub>2</sub> molecule (step 3), consistent with the outcome of isotope-labeling experiments.<sup>22</sup>

Steps (5)–(8) involve the MYW adduct and thus are completely unique to KatG. In monofunctional catalase, the

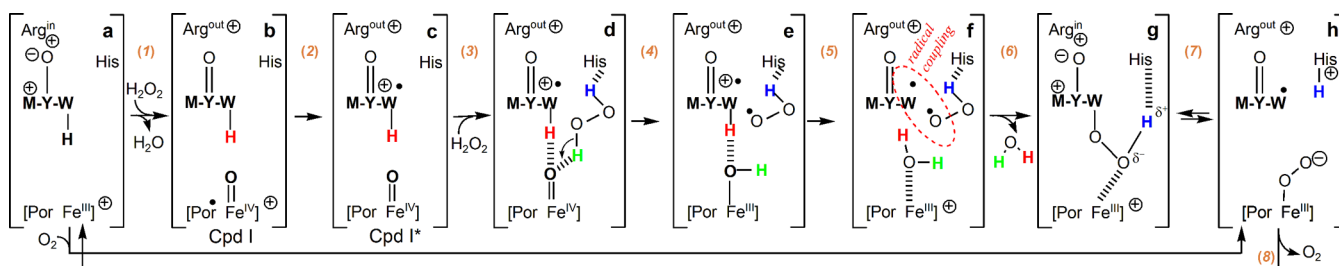


**Figure 5.** Intermediate steps in the catalase reaction of KatG (right-hand side of Figure S1). All species (a–h) were characterized by either X-ray crystallography or QM/MM calculations.

second H atom of H<sub>2</sub>O<sub>2</sub> transfers to the hydroxoferryl heme oxygen. In KatG, it is easier for the hydroxoferryl heme oxygen to capture a proton from the acidic tryptophanyl cation radical, which later reprotoates.

The swinging motion of the mobile Arg in the catalytic reaction of KatG deserves particular attention. The movement of the arginine from the *in* to the *out* conformation frees the negative charge on the oxygen of the adduct Tyr, making the MYW adduct such a good electron donor<sup>12</sup> that it delivers an electron to the heme, forming {MYW<sup>•+</sup>} (e.g., *c* in Figure 5). Formation of such a radical adduct is the key feature of the KatG catalytic cycle. In contrast, when the arginine moves in, the adduct radical disappears (e.g., *h*→*a* in Figure 5), and the Tyr charge localizes on its oxygen atom. Without the arginine, the pK<sub>a</sub> of the adduct Tyr would be so high that Tyr would remain protonated at neutral pH. As a consequence, the MYW adduct radical would not be formed, and KatG's would neither bind oxygen<sup>9</sup> nor reduce Cpd I with H<sub>2</sub>O<sub>2</sub>. Thus, it is the interplay of the arginine with the MYW adduct that imparts catalytic activity to KatG's.

In conclusion, the mechanism presented provides a consistent interpretation for all the relevant experimental and computational results available for the catalytic activity of KatG's. Catalase activity within the peroxidase framework of KatG's is possible thanks to the versatile properties of the MYW adduct in its interplay with the mobile arginine, acting as an electronic switch. This unique electronic device allows a pH-dependent control of the localization of a radical in the MYW adduct, and consequently also of the reactivity of the adduct tryptophan indole that can then be actively involved in catalysis.

## ■ ASSOCIATED CONTENT

### ● Supporting Information

Peroxidatic and catalytic reaction cycles in KatG; experimental and computational details. This material is available free of charge via the Internet at <http://pubs.acs.org>.

## ■ AUTHOR INFORMATION

### Corresponding Author

ifrcr@ibmb.csic.es; c.rovira@ub.edu

### Author Contributions

©P.C.L., X.C., and P.V. contributed equally.

### Notes

The authors declare no competing financial interest.

## ■ ACKNOWLEDGMENTS

This work was supported by a Discovery Grant 9600 from the Natural Sciences and Engineering Research Council (NSERC) of Canada (to P.C.L.), by the Canada Research Chair Program (to P.C.L.), and by grants BFU2012-36827 (to I.F.), CTQ2011-25871 (to C.R.), and 2009SGR-1309 (to I.F. and C.R.). The Canadian Light Source is supported by the NSERC of Canada, the National Research Council Canada, the Canadian Institutes of Health Research, the Province of Saskatchewan, Western Economic Diversification Canada, and the University of Saskatchewan. We acknowledge the computer support, technical expertise, and assistance provided by the Barcelona Supercomputing Center-Centro Nacional de Supercomputación (BSC-CNS).

## ■ REFERENCES

- (1) (a) Wiseman, B.; Carpena, X.; Feliz, M.; Donald, L. J.; Pons, M.; Fita, I.; Loewen, P. C. *J. Biol. Chem.* **2010**, *285*, 26662. (b) Wengenack, N. L.; Hoard, H. M.; Rusnak, F. *J. Am. Chem. Soc.* **1999**, *121*, 9748.
- (2) (a) Claiborne, A.; Fridovich, I. *J. Biol. Chem.* **1979**, *254*, 4245. (b) Singh, R.; Wiseman, B.; Deemagarn, T.; Donald, L. J.; Duckworth, H. W.; Carpena, X.; Fita, I.; Loewen, P. C. *J. Biol. Chem.* **2004**, *279*, 43098.
- (3) (a) Yamada, Y.; Fujiwara, T.; Sato, T.; Igarashi, N.; Tanaka, N. *Nat. Struct. Biol.* **2002**, *9*, 691. (b) Carpena, X.; Loprasert, S.; Mongkolsuk, S.; Switala, J.; Loewen, P. C.; Fita, I. *J. Mol. Biol.* **2003**, *327*, 475.
- (4) Poulos, T. L. *Chem. Rev.* **2014**, *114*, 3919.
- (5) (a) Vlasits, J.; Jakopitsch, C.; Bernroither, M.; Zamocky, M.; Furtmuller, P. G.; Obinger, C. *Arch. Biochem. Biophys.* **2010**, *500*, 74. (b) Jakopitsch, C.; Vlasits, J.; Wiseman, B.; Loewen, P. C.; Obinger, C. *Biochemistry* **2007**, *46*, 1183.
- (6) Singh, R.; Wiseman, B.; Deemagarn, T.; Jha, V.; Switala, J.; Loewen, P. C. *Arch. Biochem. Biophys.* **2008**, *471*, 207.
- (7) (a) Suarez, J.; Rangelova, K.; Jarzecki, A. A.; Manzerova, J.; Krymov, V.; Zhao, X.; Yu, S.; Metlitsky, L.; Gerfen, G. J.; Magliozzo, R. S. *J. Biol. Chem.* **2009**, *284*, 7017. (b) Zhao, X.; Suarez, J.; Khajo, A.; Yu, S.; Metlitsky, L.; Magliozzo, R. S. *J. Am. Chem. Soc.* **2010**, *132*, 8268. (c) Njuma, O. J.; Ndontsa, E. N.; Goodwin, D. C. *Arch. Biochem. Biophys.* **2013**, *544*, 27.
- (8) (a) Carpena, X.; Wiseman, B.; Deemagarn, T.; Herguedas, B.; Ivancich, A.; Singh, R.; Loewen, P. C.; Fita, I. *Biochemistry* **2006**, *45*, 5171. (b) Zhao, X.; Yu, H.; Yu, S.; Wang, F.; Sacchettini, J. C.; Magliozzo, R. S. *Biochemistry* **2006**, *45*, 4131. (c) Zamocky, M.; Garcia-Fernandez, Q.; Gasselhuber, B.; Jakopitsch, C.; Furtmuller, P. G.; Loewen, P. C.; Fita, I.; Obinger, C.; Carpena, X. *J. Biol. Chem.* **2012**, *287*, 32254.
- (9) Vidossich, P.; Carpena, X.; Loewen, P. C.; Fita, I.; Rovira, C. *J. Phys. Chem. Lett.* **2011**, *2*, 196.
- (10) Smulevich, G.; Jakopitsch, C.; Droghetti, E.; Obinger, C. *J. Inorg. Biochem.* **2006**, *100*, 568.
- (11) (a) Deemagarn, T.; Carpena, X.; Singh, R.; Wiseman, B.; Fita, I.; Loewen, P. C. *J. Mol. Biol.* **2005**, *345*, 21. (b) Carpena, X.; Wiseman, B.; Deemagarn, T.; Singh, R.; Switala, J.; Ivancich, A.; Fita, I.; Loewen, P. C. *EMBO Rep.* **2005**, *6*, 1156.
- (12) Vidossich, P.; Alfonso-Prieto, M.; Carpena, X.; Loewen, P. C.; Fita, I.; Rovira, C. *J. Am. Chem. Soc.* **2007**, *129*, 13436.
- (13) Alfonso-Prieto, M.; Biarnes, X.; Vidossich, P.; Rovira, C. *J. Am. Chem. Soc.* **2009**, *131*, 11751.
- (14) Singh, R.; Switala, J.; Loewen, P. C.; Ivancich, A. *J. Am. Chem. Soc.* **2007**, *129*, 15954.
- (15) (a) Colin, J.; Wiseman, B.; Switala, J.; Loewen, P. C.; Ivancich, A. *J. Am. Chem. Soc.* **2009**, *131*, 8557. (b) Zhao, X.; Khajo, A.; Jarrett, S.; Suarez, J.; Levitsky, Y.; Burger, R. M.; Jarzecki, A. A.; Magliozzo, R. S. *J. Biol. Chem.* **2012**, *287*, 37057.
- (16) Barrows, T. P.; Bhaskar, B.; Poulos, T. L. *Biochemistry* **2004**, *43*, 8826.
- (17) Blodig, W.; Doyle, W. A.; Smith, A. T.; Winterhalter, K.; Choinowski, T.; Piontek, K. *Biochemistry* **1998**, *37*, 8832.
- (18) (a) Tommos, C.; Skalicky, J. J.; Pilloud, D. L.; Wand, A. J.; Dutton, P. L. *Biochemistry* **1999**, *38*, 9495. (b) Baugher, J. F.; Grossweiner, L. I. *J. Phys. Chem.* **1977**, *81*, 1349. (c) Zhang, M.-T.; Hammarström, L. *J. Am. Chem. Soc.* **2011**, *133*, 8806.
- (19) (a) Carloni, P.; Rothlisberger, U.; Parrinello, M. *Acc. Chem. Res.* **2002**, *35*, 455. (b) Rovira, C. *WIREs Comput. Mol. Sci.* **2013**, *3*, 393.
- (20) Vidossich, P.; Alfonso-Prieto, M.; Rovira, C. *J. Inorg. Biochem.* **2012**, *117*, 292.
- (21) Jakopitsch, C.; Wanasinghe, A.; Jantschko, W.; Furtmuller, P. G.; Obinger, C. *J. Biol. Chem.* **2005**, *280*, 9037.
- (22) Vlasits, J.; Jakopitsch, C.; Schwanninger, M.; Holubar, P.; Obinger, C. *FEBS Lett.* **2007**, *581*, 320.